ELSEVIER

Journal of Nuclear Materials 273 (1999) 52–59

journal of nuclear materials

www.elsevier.nl/locate/jnucmat

The effect of texture variation on delayed hydride cracking behavior of Zr–2.5%Nb plate

Sung Soo Kim *, Sang Chul Kwon, Young Suk Kim

Korea Atomic Energy Research Institute, P.O. Box 105, Yousung-Ku, Taejon 305-353, South Korea

Received 23 July 1998; accepted 28 December 1998

Abstract

In order to investigate the effect of texture variation on the delayed hydride cracking behavior in Zr–2.5%Nb plates, crack growth rate and K_{IH} tests have been carried out at temperature ranges varying from 415 to 506 K after texture modification by rolling. The texture variation of plates was achieved by direct-rolling and cross-rolling. Texture was measured through the determination of inverse pole figures, from which the basal pole components were calculated. The results have shown that the texture of a plate in which the basal poles are concentrated in the transverse direction can be changed significantly by cross-rolling. The crack growth rate increases exponentially with the basal pole component in the direction normal to the cracking plane. The increase in stress relieving temperature on cold worked material reduces crack growth rate. K_{IH} decreases linearly with the basal pole component, and a behavior of which could be explained by the uniformly dispersed aggregate composite theory.

1. Introduction

The Zr–2.5%Nb alloy is extensively used in the pressure tubes of CANDU reactor because of its high strength, corrosion resistance, and low neutron capture cross section [1]. However, a number of pressure tubes have been re-tubed in Canada due to unexpectedly large 'in-reactor' deformation caused by fast neutron irradiation [2], and coolant leak accidents caused by delayed hydride cracking (DHC), which is related to hydrogen content, residual and applied stress, and the presence of flaws [3–5]. The problem of elongation has been mitigated through design improvements recently. DHC still remains as a primary concern but probability has been reduced at rolled joint through application of zero clearance joints on the integrity of pressure tubes to the present [2,6].

Pressure tube material absorbs the hydrogen produced by corrosion processes during reactor operations, and the excess hydrogen over terminal solid solubility (TSS) precipitates as a brittle hydride, whose fracture toughness is given by $K_{IC} = 1$ to 3 MPa m^{-1} [5]. Because hydrogen movement by the interstitial diffusion mechanism is very fast, hydrogen precipitates as Zr-hydride in the tri-axial stress field in front of a crack tip, and then the hydride fractures when the length of the hydride reaches the critical crack length. Thus, crack growth by DHC mechanisms has time and temperature dependencies, since the crack grows through repetition of the growth and fracture of Zr-hydride, and the growth rate is affected by the shape of the flaw, the stress state, and the microstructure of the material [8]. The microstructure of materials involve texture, dislocation density, and the relative amount and configuration of α-Zr and β-Zr, which can affect hydrogen movement, hydride precipitation, and hydride growth in a given materials.

Coleman et al. [8,9] have investigated the effects of texture on DHC behavior for a Zr–2.5%Nb alloy. They have shown that when the basal pole component, F, is high in the loading direction, K_{IH} is low and the crack growth rate is fast in materials having limited ranges of the basal pole component, i.e. $F = 0.06$ and $F = 0.62$ for pressure tubes and $F = 0.16$ to 0.17 and $F = 0.67$ for plates. However the effects of gradual texture variation on DHC behavior are not clearly understood yet.

* Corresponding author. Tel.: +82-42 868 2061; fax: +82-42 868 8346; e-mail: sskim6@nanum.kaeri.re.kr.

0022-3115/99/$ – see front matter
PII: S0022-3115(99)00017-3

The objective of the present work was to systematically investigate and understand the effect of gradual texture variation on DHC behavior. Thus, differently textured Zr–2.5%Nb plates having a wide range of basal pole components (F) were obtained by direct-rolling and cross-rolling, and crack growth rate and K_{IH} tests were carried out over a temperature range of 415–506 K. The relationship between F and K_{IH} and between F and the crack growth rate were derived experimentally and discussed.

2. Experimental

Hot-rolled and annealed Zr–2.5%Nb plates A (thickness: 4.6 mm) and B (thickness: 6.6 mm) supplied by Teledyne Wah Chang Albany were used in the texture modification by cold rolling. The chemical composition of the plates is shown in Table 1. Direct-rolling and cross-rolling rotated 90° from the original rolling direction were used to modify the texture of the plates. The amount of cold work was selected as 30% (true strain), similar to that of the CANDU pressure tubes [1,10].

The subsized compact tension (CT, $W = 17$ mm) specimens were machined according to ASTM E-399 from the four differently textured plates. T–L specimens with cracking planes perpendicular to the transverse direction and parallel to the longitudinal direction of the plate were machined from all plates, and some L–T specimens were prepared from the cross-rolled plate A. The original notation of the plate was used for identification even after the cross-rolling.

Hydrogen was charged electrolytically, and the hydrided specimens were homogenized and stress relieved at 640 K for 24 h. The hydrogen content of the hydrided specimens was about 200 ppm. Some specimens machined from plate A were homogenized and stress relieved at 740 K and 773 K for 24 h. The texture variations by direct- and cross-rolling were observed through the measurement of inverse pole figures for 17 poles using Cu-Kα radiation [11]. The basal pole component, F, which represents the resolved fraction of the basal planes in the direction of interest, was calculated by the method proposed by Evans et al. [12]. The basal pole component is defined by Eq. (1)

$$F = \sum V_\alpha \cos^2\alpha, \qquad (1)$$

where α is the angle between the basal pole of the grain and the direction of interest, and V is the volume fraction of grains tilted at angle α.

The hydrided CT specimens were fatigue precracked according to ASTM E-399. The crack growth rate and K_{IH} tests were performed using a lever arm tester with an initially applied $K_I = \sim 15$ MPa m^{-1} in the temperature range of 415–506 K after the thermal cycle of 603 K for 1 h. The accurate K_I was recalculated with the measured crack length, and the applied K_I ranges were found to be $K_{IH} = 15$ to 20 MPa m^{-1} for all T–L specimens, and $K_I = 20$ to 26 MPa m^{-1} for L–T specimens in plate A.

The DC potential drop method was used to monitor the crack advance, and the average crack growth rate was determined with the assumption that the crack growth rate was constant in the range of applied K_I. K_{IH} was measured using the load reducing method, and the K_I in which the crack did not grow for at least 24 h was defined as K_{IH}, as Sagat et al. [13].

3. Results

The grains of both the direct-rolled and cross-rolled plates were elongated in the longitudinal direction, and were more wavy in the cross-rolled than in the direct rolled plates A and B. The average grain size was about 10 μm in length, 1–2 μm in thickness, and 5 μm in width in plate A, and 20 μm in length, 1–2 μm in thickness, and 5 μm in width in plate B. The grain size was not changed much by direct-rolling or cross-rolling.

The inverse pole figures for plates A and B are shown in Figs. 1 and 2 respectively. The basal poles were concentrated in the transverse direction of the as-received plate A, as shown in Fig. 1 (a). The basal pole component in the transverse direction of plate A was decreased and that in the normal direction was increased by cross-rolling, as shown in Fig. 1(b) and (c). Most of the basal poles in both direct-rolled and cross-rolled plates B were concentrated in the normal direction, and the maximum density of the basal pole was observed in directions tilted ±25° from the normal direction.

Even though the texture of plate A was changed significantly by cross-rolling, that of plate B was not. This could be understood by the following explanation. The (0 0 0 2) poles are concentrated strongly in the

Table 1
Chemical compositions of as-received Zr–2.5%Nb plates A and B (wt%)

Plates	Elements							
	Nb	H	C	N	O	Fe + Cr	Hf	Zr
Plate A	2.7	0.001	0.02	0.005	0.14	0.13	0.04	Bal.
Plate B	2.52	0.006	0.02	0.005	0.15	0.13	0.04	Bal.
Specification max.	2.0–3.0	0.005	0.05	0.025	0.18	0.2	4.5	>95.5

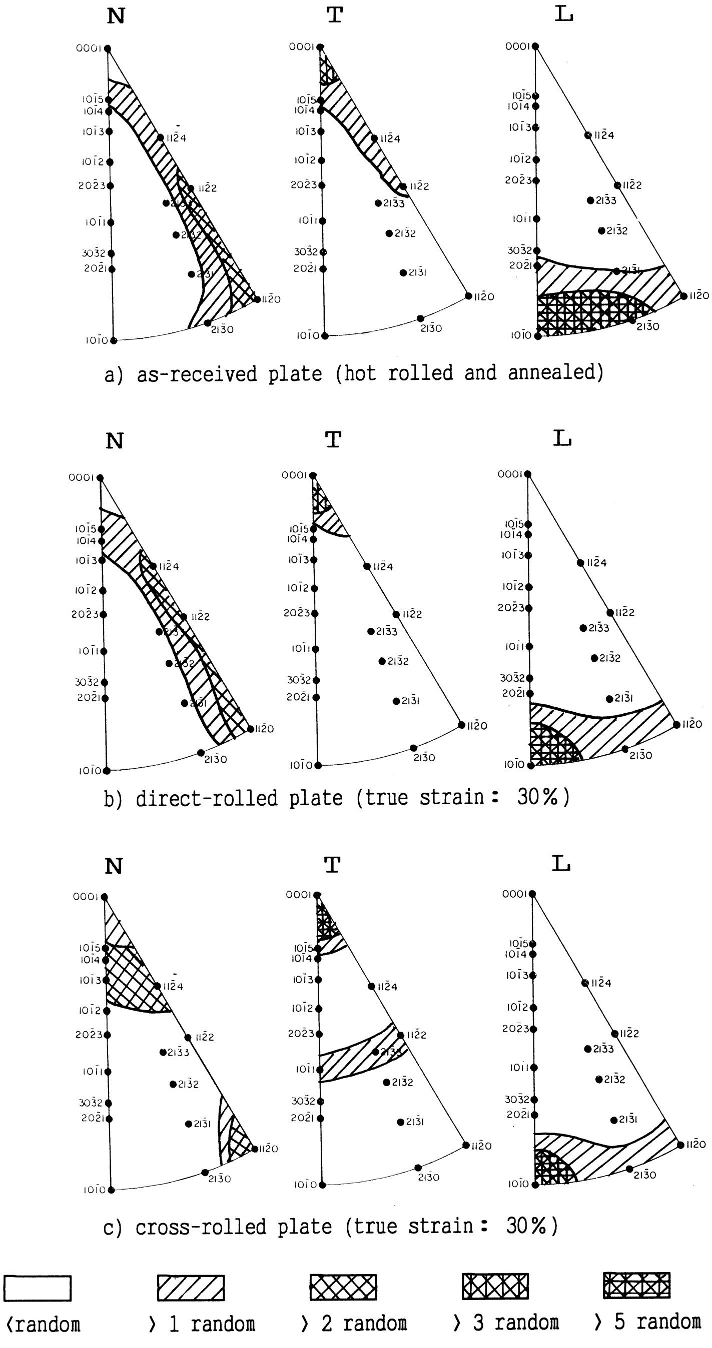

Fig. 1. Inverse pole figures for plate A, (a) as-received plate (hot rolled and annealed), (b) direct-rolled plate (true strain: 30%), (c) cross-rolled plate (true strain: 30%).

transverse direction in the plate A as shown in the middle of Fig. 1(a). Cross-rolling means that the rolling direction in the cross-rolling operation becomes transverse direction of the original plate. Thus, the tensile stress is applied in the [0 0 0 2] direction of grains in the plate A during the cross-rolling process.

It is known that there are no available deformation mechanisms except twinning when the stress is applied in [0 0 0 2] direction of the crystal. Therefore, texture can be changed significantly in plate A, not in plate B, because (0 0 0 2) poles are not concentrated in plate B as shown in the middle of Fig. 2(a). Usually, strong cold

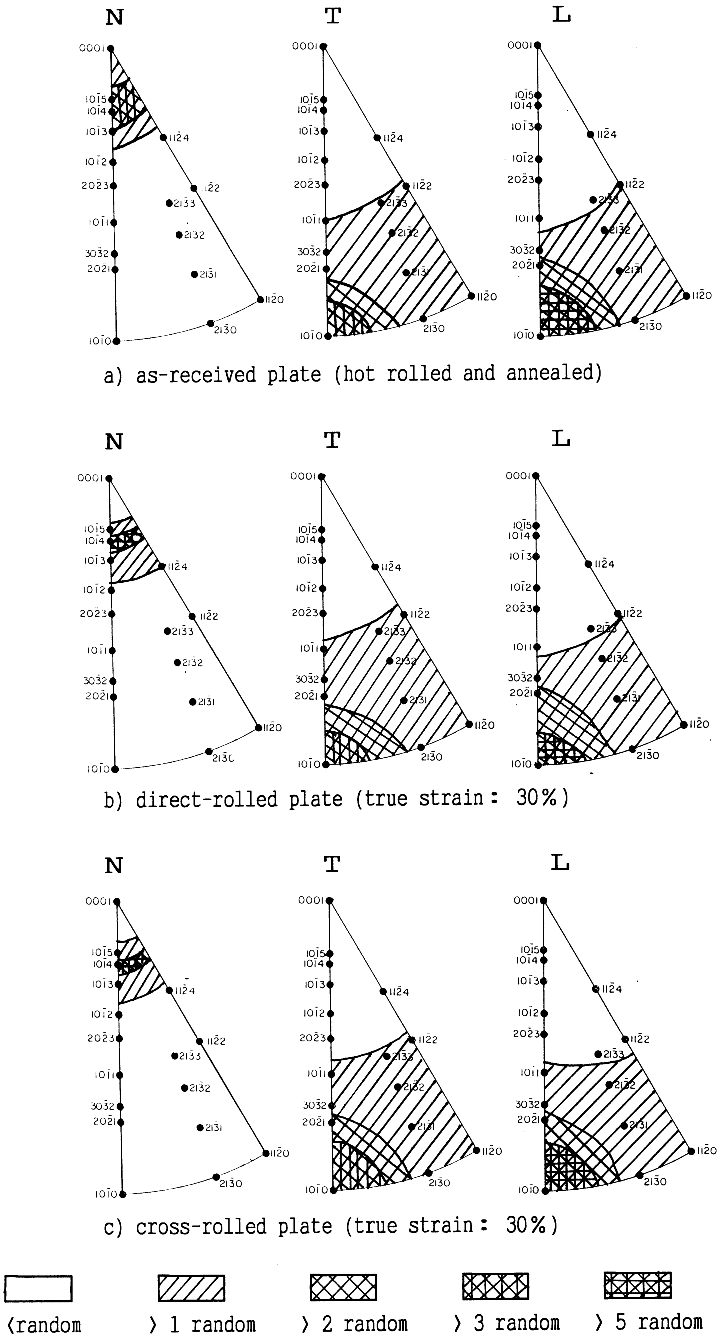

Fig. 2. Inverse pole figures for plate B, (a) as-received plate (hot rolled and annealed), (b) direct-rolled plate (true strain: 30%), (c) cross-rolled plate (true strain: 30%).

rolling or cross-rolling gives texture with concentrated basal pole in the normal direction of the plate. The original texture of the plate B has already concentrated basal pole in the normal direction as well as strong (1 0 1 0) pole in the longitudinal direction. It seems there is little room for the plate B to change its texture during further rolling.

The basal pole components calculated from the texture coefficient are shown in Table 2. The basal pole component in the transverse direction of the direct-rolled

Table 2
Basal pole components for various Zr–2.5%Nb plates used in this study

Materials	Direction		
	Normal	Transverse	Longitudinal
Plate A			
As-received	0.42	0.54	0.04
30% cross-rolled	0.54	0.39 [a]	0.07 [a]
30% direct-rolled	0.41	0.53	0.06
Plate B			
As-received	0.66	0.19	0.15
30% cross-rolled	0.71	0.14 [a]	0.15 [a]
30% direct-rolled	0.69	0.18	0.13

[a] Transverse and longitudinal directions are for those of the original plate.

plate A was $F_T = 0.53$ and that of the cross-rolled plate A was $F_T = 0.39$, and those of the direct-rolled and cross-rolled plates B were $F_T = 0.18$ and $F_T = 0.14$, respectively.

The crack growth rates for the various textured plates were plotted against the reciprocal temperature in Fig. 3. The crack growth rate exhibited an Arrhenius relationship, and the apparent activation energy values were $Q = 38$ to 42 kJ/mol in the differently textured plates.

The crack growth rate of the direct-rolled T–L specimen in plate A ($F_T = 0.53$) was about two times higher than that of the cross-rolled one ($F_T = 0.39$), and was about six times higher than that of the cross-rolled L–T specimen ($F_T = 0.07$) at the same temperature. The rate of the direct-rolled T–L specimen in plate B was about 50% higher than that of the cross-rolled one. Thus, it seems that the crack growth rate was decreased by a decrease in basal pole components in the direction normal to the cracking plane in plate A or B.

The crack growth rates for various textured plates at 473 K are plotted against the basal pole components in Fig. 4. The crack growth rate in plate A increased exponentially with the basal pole components. Even though the basal pole components in plate B were lower than those of plate A, the crack growth rates were higher than those of plate A. This means that crack growth may be affected by some factors except texture, although texture has a great effect on DHC. One of these factors may be grain shape since it is known that the diffusion in the grain boundary is much higher than that in the lattice.

The variation of the crack growth rate with increases in the stress relieving temperature in plate A is shown in Fig. 5. The crack growth rates of both the direct-rolled and cross-rolled specimens treated at 740 K for 24 h and 773 K for 24 h were reduced to 2/3 and 1/3, respectively, of the crack growth rate of specimens treated at 640 K for 24 h.

The threshold stress intensity factor, K_{IH}, for the variously textured plates with basal pole components in

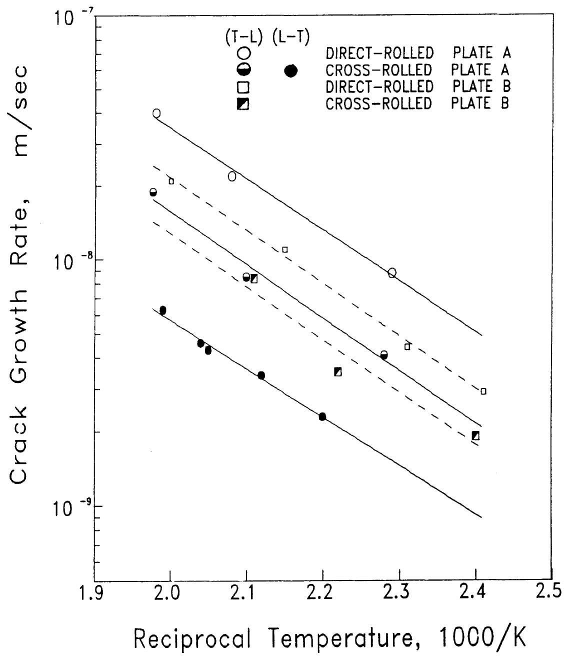

Fig. 3. Crack growth rate reciprocal temperature in plates A and B.

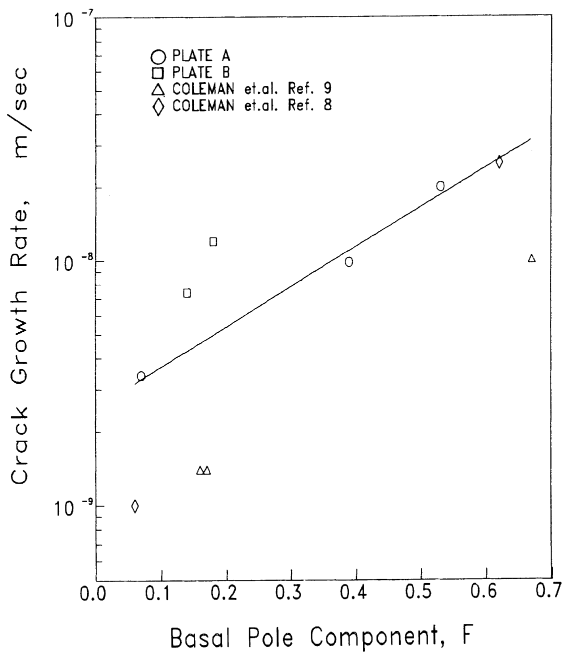

Fig. 4. Crack growth rate at 473 K with basal pole component in plates A and B.

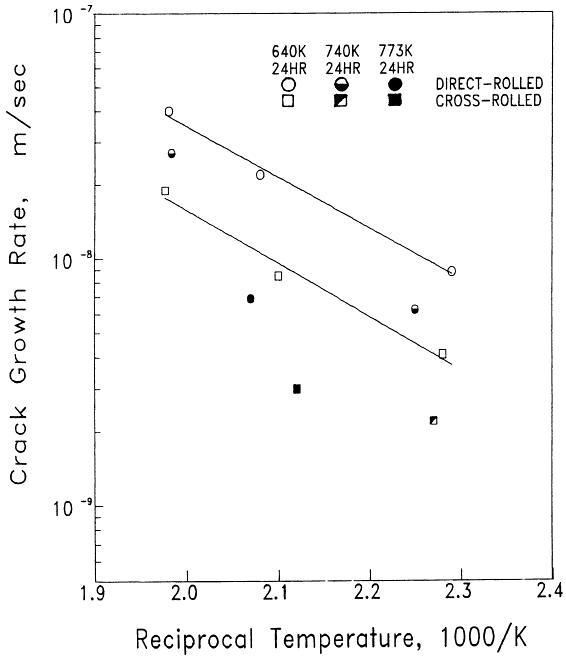

Fig. 5. Effects of stress relieving temperature on crack growth rate in plate A.

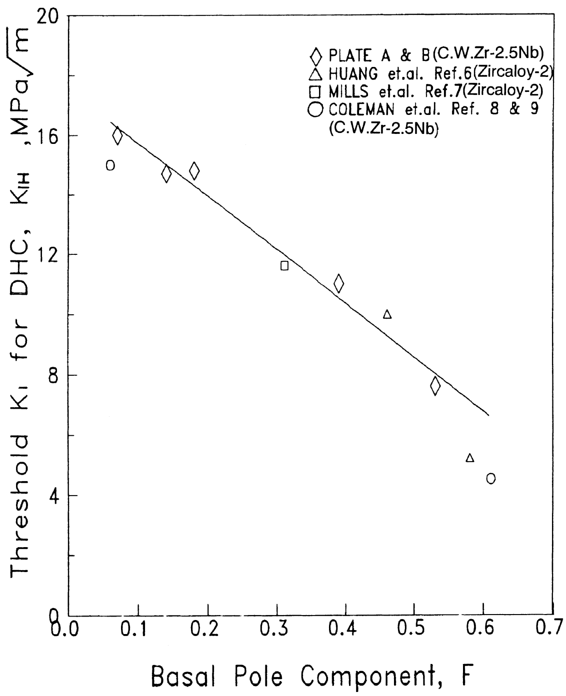

Fig. 6. Threshold stress intensity factor with basal pole component in plate A and B.

the direction normal to cracking plane are shown in Fig. 6. K_{IH} decreased with an increase in F, and the relationship between K_{IH} and F was empirically obtained in the range of $F = 0.07$ to 0.53.

$$K_{IH} = C_1 - C_2 \times F, \tag{2}$$

where K_{IH} is in MPa m^{-1}, C_1 and C_2 are constants of 17.5 MPa m^{-1} and 17 MPa m^{-1}, respectively, for plates A and B, and F is the basal pole component in the direction normal to the cracking plane. The constant, C_1, means the fracture toughness of hydride when F is 0.

4. Discussion

4.1. Crack growth rate

The results have shown that the crack growth rate increases with an increase in the basal pole components in the direction normal to the cracking plane. This behavior could be explained by the concept of the DHC mechanism. Because it is reported that the fracture toughness of the Zr-hydride is $K_{IC} = 1$ to 3 MPa m^{-1} [5] and the interplanar angle between the basal plane and the most common hydride habit plane is 14.7°, as the basal pole components increase, the number of grains susceptible to the precipitation of the hydride increases, and the crack can then propagate fast through the rapid growth and fracture of the hydride. This behavior is consistent with results obtained by Huang et al. [6,7] and Coleman et al. [8,9].

Although the K_I range tested for L–T specimens was somewhat higher than that for T–L specimens, the crack growth rate, da/dt at 473 K in plate A increased exponentially with the basal pole component, and showed an Arrhenius temperature dependency. Thus

$$\frac{da}{dt} = C_1 \exp(C_2 \times F) \exp(-Q/RT), \tag{3}$$

where C_1 is a constant which represents the microstructural factor, C_2 is a constant for the texture dependency of crack growth, Q is the apparent activation energy, R is the gas constant, and T is the absolute temperature. The measured apparent activation energy, $Q = 38$ to 42 kJ/mol, is consistent with the results obtained by Coleman et. al. [14] in DHC tests on Zr–2.5%Nb pressure tubes and with the results obtained by Skinner [15] in hydrogen diffusion anneal tests on Zr–2.5%Nb pressure tubes. Thus, hydrogen diffusion in α-Zr with an activation energy of $Q = 38$ to 42 kJ/mol is believed to be the major mechanism for hydride growth during DHC. The texture does not seem to affect the DHC mechanism.

The constants C_1 and C_2 for plate A appeared to be 2.6×10^{-9} m/s and 3.7, respectively, and those from Coleman's results [9] for the warm cross-rolled plate were calculated to be $C_1 = 6.9 \times 10^{-10}$ m/s and $C_2 = 4$

(Fig. 4). C_2 is very similar for plate A and the warm cross-rolled plate, whereas the values of C_1 are different. This difference seems to be due to the microstructural difference caused by the different thermomechanical treatments, i.e. the cold-worked and stress relieving treatment vs the warm cross-rolled treatment.

Coleman et al. [4,9] have reported that crack growth rate increases with yield strength through the enhancement of the hydrogen diffusion to the crack tip due to the higher stress concentration. The yield strength at room temperature in specimens stress-relieved at 640 K for 24 h increases with the basal pole components, in plates A and B, as shown in Fig. 7, and the relationship is as follows:

$$\sigma_{YS} = 630 + 288 \times F, \tag{4}$$

where σ_{YS} is the room temperature yield strength in unit MPa, and F is the basal pole component in the direction parallel to the tensile axis. Therefore, it is thought that the increase in basal pole components increases the crack growth rate through the effects of not only hydride precipitate increases, but also yield strength increases.

Stress relieving treatments at higher temperatures lowered the crack growth rate. Since Zr–2.5%Nb alloy pressure tube material is usually used in a two phase state of α-Zr (HCP) + β-Zr (BCC) [9] and the diffusivity of the β-Zr phase is about two orders of magnitude higher than that of the α-Zr phase [15,16], the morphology of the β-Zr phase affects the hydrogen mobility in bulk materials, causing the crack growth rate to change. Since the β-Zr phase decomposition reaction occurs through a substitutional diffusion mechanism, this reaction can be enhanced highly by increasing the stress relieving temperature. Thus, the effect of the decrease in crack growth rate with temperature seems to be due to a reduction in hydrogen mobility through a decrease in the number of lattice defects and the morphology change of β-Zr.

Therefore, this treatment can be used to manufacture DHC resistant Zr–2.5%Nb pressure tubes, although the yield strength is somewhat lowered by this process. However, because Zr–2.5%Nb pressure tubes in nuclear reactors are exposed to fast neutrons, the microstructure of the pressure tube material would change during service, and the crack growth rate would increase. Thus, this treatment would be very effective to non-nuclear components only. However, starting from a lower baseline by breaking up the β-Zr in advance may still provide some benefit when the material is irradiated.

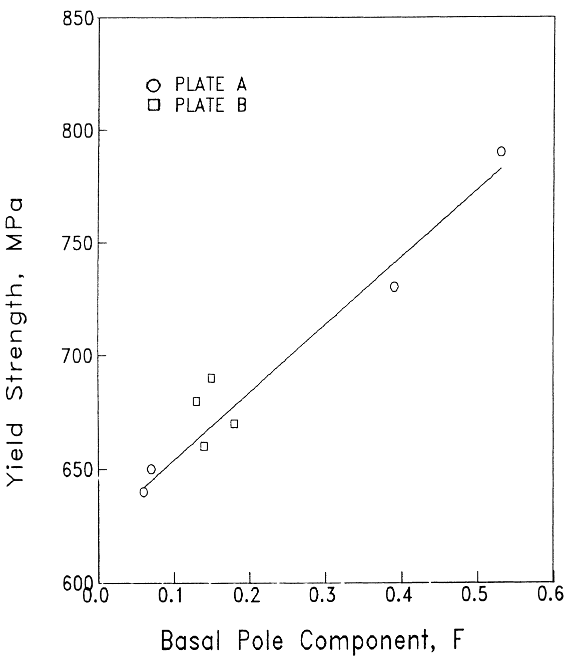

Fig. 7. Room temperature yield strength with basal pole component in plate A and B.

4.2. Threshold stress intensity factor (K_{IH})

The threshold stress intensity factor, K_{IH} decreased linearly with the basal pole component in the range of $F = 0.07$ to 0.53. This is consistent with the results reported by Coleman et al. [9,13]. The K_{IH} values for Zr–2.5%Nb and Zircaloy-2 [6,9] are plotted together in Fig. 6. No significant difference exists in K_{IH} between Zr–2.5%Nb and Zircaloy-2. This seems to be attributable to the fact that the major matrix phase is α-Zr in both alloys.

K_{IH} is one of the necessary criteria for crack initiation by the DHC mechanism. K_{IH} values are reported in a small range rather than as a unique value [6,7,9]. This seems to be due to the microstructural variations between specimens. However, if conservatism is chosen as a primary factor in the flaw assessment, the lower value of K_{IH} should be used to decide whether the crack will initiate or not. In this case, the lower bounding value of K_{IH} would be important.

Because crack growth by DHC is achieved by repetition of hydride precipitate growth and fractures at the crack-tip, hydrided Zr-alloys can be thought of as composites composed of ductile matrix grains where the basal poles are nearly parallel to the cracking plane, and brittle grains where the basal poles are nearly perpendicular to the cracking plane. Thus, the decreasing behavior of K_{IH} with the basal pole components can be interpreted as a uniformly dispersed aggregate composite by the rule of mixture [17]. If F can be used as a volume fraction susceptible to DHC and $(1 - F)$ can be used as a volume fraction of the ductile matrix, K_{IH} can be expressed as follows:

$$K_{IH} = F \times K_{IC\text{ of Zr-hydride}} + (1 - F) \times K_{IC\text{ of hydrided matrix}}, \quad (5)$$

where $K_{IC\text{ of Zr-hydride}}$ is the fracture toughness of Zr-hydride, which is given by $K_I = 1$ to 3 MPa m^{-1}, and $K_{IC\text{ of hydrided matrix}}$ is the fracture toughness of matrix grain non-susceptible to DHC. $K_{IC\text{ of hydrided matrix}}$ is calculated as $\sim$18 MPa m^{-1} at $F = 0$ in Fig. 6, which is lower than the $K_{IC} = \sim$25 MPa $^{m-1}$ at $F = \sim$0.61 reported in references [18–20]. Although the calculated values are dependent on the $K_{IC\text{ of hydrided matrix}}$ value, the decreasing trend of K_{IH} with F can be properly explained by Eq. (5).

The increase in K_{IH} with F would increase the allowable crack depth in the Zr-alloy components, and there is a relationship between K_{IH} and the circumferential allowable crack depth which does not grow through the DHC mechanism [14]

$$a = C \times (K_{IH}/\sigma H)2, \quad (6)$$

where a is the crack depth in mm, C is a constant, K_{IH} is in MPa m^{-1}, and σ_H is the applied stress in MPa. Thus, an increase in K_{IH} through a texture variation could provide additional tolerance for DHC in Zr-alloy components.

5. Conclusions

1. The texture of plates in which the basal poles are concentrated in the transverse direction can be modified significantly by cross-rolling.
2. The crack growth rate increases exponentially with the basal pole component, F, and an Arrhenius-type temperature dependency. Thus the rate can be expressed as follows

$$\frac{da}{dt} = C_1 \exp(C_2 \times F) \exp(-Q/RT).$$

3. K_{IH} decreases linearly with the basal pole component, F, and the decreasing behavior of K_{IH} with F can be reasonably interpreted as a composite concept by the rule of mixture.

Acknowledgements

This work has been carried out as a PHWR Pressure Tube Material Project of the Nuclear R&D program funded by the Ministry of Science and Technology. The authors acknowledge Professor B. Cox of University of Toronto and Dr. J.H. Hong of Korea Atomic Energy Research Institute for their helpful discussions.

References

[1] E.F. Ibrahim, B.A. Cheadle, Can. Metall. Q. 24 (1985) 273.
[2] G.J. Field, J. Nucl. Mater. 159 (1988) 3.
[3] C.E. Coleman, J.F.R. Ambler, Rev. Coatings Corros. III (1979) 105.
[4] G.K. Shek, D.B. Graham, Zirconium in the Nuclear Industry: Eighth International Symposium, ASTM STP 1023 (1989) 89.
[5] L.A. Simpson, C.D. Cann, J. Nucl. Mater. 87 (1979) 303.
[6] F.H. Huang, W.J. Mills, Metall. Trans. A 22A (1991) 2060.
[7] W.J. Mills, F.H. Huang, Eng. Frac. Mech. 39 (1991) 241.
[8] C.E. Coleman, Zirconium in the Nuclear Industry: Fifth Conference, ASTM STP 754 (1982) 393.
[9] C.E. Coleman, S. Sagat, K.F. Amouzouvi, Control of Microstructure to Increase the Tolerance of Zirconium Alloys to Hydride Cracking, Atomic Energy of Canada Limited Report AECL-9524 (1987).
[10] B.A. Cheadle, C.E. Coleman, H. Licht, Nucl. Tech. 57 (1982) 413.
[11] J.E. Winegar, Measurement of crystallographic texture at chalk river nuclear laboratories, Atomic Energy of Canada Limited Report AECL-5626 (1977).
[12] W.M. Evans, R.F. Gessner, J.G. Goodwin, Metall. Trans. 3 (1972) 2879.
[13] S. Sagat, C.E. Coleman, M. Griffiths, B.J.S. Wilkins, Zirconium in the Nuclear Industry: Tenth International Symposium, ASTM STP 1245 (1994) 35.
[14] C.E. Coleman, J.F.R. Ambler, Zirconium in the Nuclear Industry, ASTM STP 633 (1977) 589.
[15] B.C. Skinner, R. Dutton, Hydrogen effects of material behavior, in: Neville R. Moody, Anthony W. Thomson (Eds.), The Minerals, Metals and Materials Society, 1990, pp. 73–83.
[16] K.F. Amouzouvi, L.J. Clegg, Metall. Trans. A 18A (1987) 1687.
[17] G.E. Dieter, Mechanical Metallurgy, 3rd ed., McGraw-Hill, New York, 1986.
[18] A.C. Wallace, G.K. Shek, O.E. Lepik, Zirconium in the Nuclear Industry: Eighth International Symposium, ASTM STP 1023 (1989) 66.
[19] L.A. Simpson, C.W. Chow, Zirconium in the Nuclear Industry: Seventh International Symposium, ASTM STP 939 (1987) 579.
[20] C.K. Chow, L.A. Simpson, Case histories involving fatigue and fracture mechanics, ASTM STP 918 (1987) 78.